

Thermalization of Isolated *BEC* Under a *PT*-Symmetric Environment

Javed Akram,^{1,*} Asad Hussain,¹ Muhammad Nouman,¹ and Jameel Hussain²

¹*Department of Physics, COMSATS University Islamabad, Islamabad Pakistan*

²*Department of Electronics, Quaid-i-Azam University, Islamabad, Pakistan*

(Dated: November 2, 2022)

The postulates of the eigenstate thermalization hypothesis (*ETH*) expresses that the thermalization occurs due to the individual eigenstate of the system's Hamiltonian. But the *ETH* put no light on the dynamics that lead toward the thermalization. In this paper, we observe the thermalization of a Bose-Einstein Condensate (*BEC*) confined in an optical lattice potential that is embedded on the harmonic trap. Such optical lattice potential offers local friction to the oscillating *BEC*. The spread in the temporal density plot of *BEC* shows the thermalization of the *BEC*. Moreover, we observe that the presence of a *PT*-symmetric potential greatly influences the *BEC* dynamics and the thermalization of the system. The presence of a *PT*-symmetric potential offers a way to manipulate the mean position of the *BEC* to a desire location and for a desired length of time.

I. INTRODUCTION

Confirmation of long-standing diverse ideas of condensed matter physics begins with the first realization of Bose-Einstein condensates (*BECs*) of dilute atomic gases [1–4]. Among those ideas included the nature of superfluidity, the critical velocity for the beginning of the dissipation [5, 6], quantization of vortices [7–9], the generation and dynamics of soliton waves [10–13], and the impact of impurities for different practical applications [10, 11, 14]. Recently it also leads to probe the long-standing question of thermalization of an isolated quantum system both theoretically and experimentally [15–17]. In these studies, the thermalization observed in double-well potential confinement under the influence of Josephson interaction [15], and it was also investigated experimentally in an optical lattice environment [17].

In this paper, we study the thermalization of *BEC* in harmonic trap embeds with optical lattice potential. We also investigate the impact of a *PT*-symmetric periodic potential on the thermalization of the *BEC*. We initially trapped *BEC* in a harmonic trap after achieving the equilibrium, we shift the harmonic potential minima for time $t > 0$. At the same time, we switched on the optical lattice which is embedded in the harmonic trap. Such a lattice potential offers friction for the dipole oscillations of the *BEC*. The idea of *PT*-symmetric potential represents the scenario in which there are alternative gain and lost regions in an optical lattice, e.g, as explained for double-well confinement [18]. In an optical lattice, the transmission between adjacent wells is controlled by controlling the tunneling between the wells. The periodic lattice potential here acts as a medium that absorbs the partial kinetic energy and partial potential energy of the *BEC* entropy. That medium helps in bringing the *BEC* into thermal equilibrium. Furthermore, we also test the localization and thermalization of *BEC* under a periodic *PT*-symmetric environment. The idea of non-Hermitian Hamiltonian obeying *PT*-symmetry was introduced by Bender and Boettcher [19] and this appears as an exten-

sion to quantum mechanics from a real to the complex domain. The *PT*-symmetric conditions are more physical than the earlier strict mathematical condition of hermiticity of the Hamiltonian for real eigenvalues. The operator "*P*" and "*T*" represent parity reflection and time reversal, respectively. The operator *P* acts on position and momentum operator as $P: x \rightarrow -x, p \rightarrow -p$ and the time operator *T* acts on position and momentum operator as $T: x \rightarrow x, p \rightarrow -p, \text{ and } i \rightarrow -i$. The remaining part of this paper is organized as follows. In Sec. II, we describe the working models, like analytical, numerical, and Ehrenfest methods. Where we discuss all the relevant issues. In Sec. III, we discuss our results, figures for the *BEC* dynamics through a periodic potential embedded on a harmonic confining potential. Moreover, we also discuss the impact of the *PT*-symmetric system over the thermalization of the *BEC*. We observe the impact of the complex part of the potential in the *PT*-symmetric Hamiltonian. Conclusion comes in Sec. IV, with the future suggestions for the related research, and we compare the *BEC* dynamics with and without the *PT*-symmetric.

II. THEORETICAL MODELS

To accurately model an elongated *BEC*, we use a dimensionless quasi-1D Gross-Pitaevskii equation (GPE) [20]. The dimensionless equation can be achieved by taking time t in ω_x^{-1} , and scale length $L = \sqrt{\hbar/m\omega_x}$ in terms of harmonic oscillator length along x -axis and energy is scaled by $\hbar\omega_x$,

$$i \frac{\partial \psi(x, t)}{\partial t} = \left[-\frac{1}{2} \frac{\partial^2}{\partial x^2} + U(x) + g_s |\psi|^2 \right] \psi(x, t), \quad (1)$$

where $\psi(x, t)$ as a dimensionless macroscopic wavefunction of the *BEC*, t and x stands for time and 1D-space space coordinate, respectively. Here, we use normalized wavefunction such as, $\int |\psi(x, t)|^2 dx = 1$. The 1D interaction strength is given as $g_s = 2N\omega_r a_s / (\omega_x L)$, where a_s

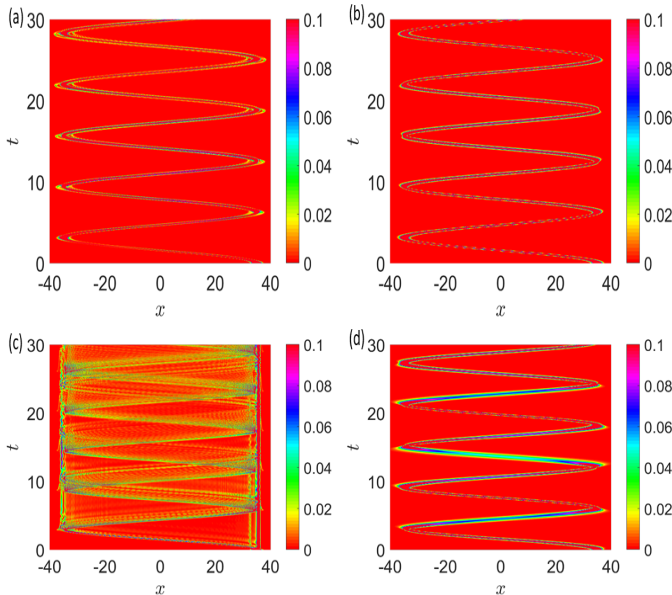


FIG. 1: (Color online) Comparison of numerical results (left column) and analytical results (right column) of *BEC* temporal density. The others dimensionless parameters are, interaction strength $g_s = 3$, initial mean-position of the *BEC* defines as $x_0 = 35$. Here, in upper row the optical periodic potential is $V_0 = 5$ and in the lower row it consider as $V_0 = 50$.

describes the s-wave scattering length [11], the number of atoms in *BEC* is represented by N , ω_r stands for the radial frequency component of the harmonic trap [10]. To study the thermalization and dipole oscillation for an isolated *BEC*, we purpose the trapping potential $U(x)$,

$$U(x) = V(x) + \iota W(x), \quad (2)$$

where the real part of the potential defines as $V(x) = x^2/2 + V_0 \cos^2(x)$, here the first term represents the dimensionless harmonic potential confinement, second term models the periodic lattice potential of the system, which serves as an optical lattice of strength V_0 and offers friction to the *BEC* during its dipole oscillation. The complex part, $W(x) = W_0 \sin(x)$ compensates the gain and loss of the *BEC* atoms, such potentials makes our system a non-Hermitian system. However, this special potential follows the *PT*-symmetric condition. Here $W(x) < 0$ represents the loss of atoms and $W(x) > 0$ describes the gain of the *BEC* atoms.

A. Analytical method

The solution of time dependent *GPE* by a variational approach [21–24] can help to extract the qualitative and quantitative information about the system. The variational approach relies on the initial choice of the trial

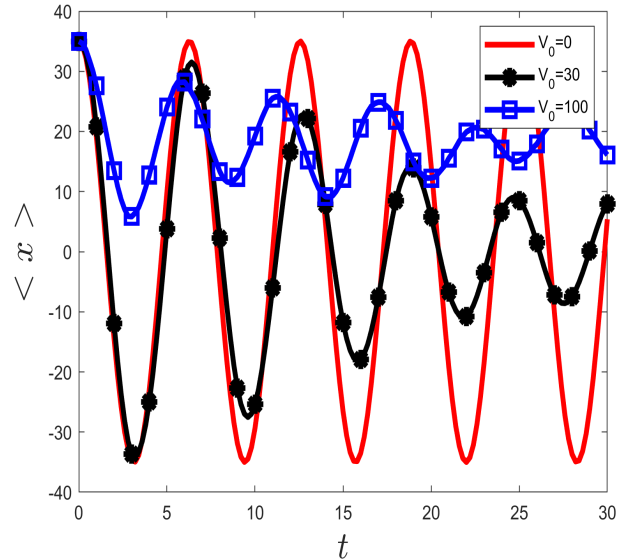


FIG. 2: (Color online) The dimensionless mean position of the *BEC* versus the dimensionless time for different periodic potentials V_0 . Other dimensionless parameters are $W_0 = 0$, $g_s = 3$ and the initial mean position of the *BEC* is $X_0 = 35$.

wave function. In our case, we use Gaussian shape wave-function with time dependent variables. This approach helps us to find second order ordinary differential equations for the time dependent variables. Which in turn characterize the dynamics of the *BEC*. Here, we let the initial ansatz as

$$\psi(x, t) = \frac{1}{\sqrt{a(t)}\sqrt{\pi}} e^{-\frac{(x-x_0(t))^2}{2a(t)^2} + ix\alpha(t) + ix^2\beta(t)}, \quad (3)$$

above ansatz is a Gaussian distribution centered at $x_0(t)$. Here, x is defined as the dimensionless space coordinate, $x_0(t)$ describes the dimensionless mean position of the *BEC*, $a(t)$ tells us about the dimensionless width of the *BEC*, $\alpha(t)$ and $\beta(t)$ are the variational parameters. To find all the unknown variational parameters, we let the Lagrangian density of our system as,

$$\mathcal{L} = \frac{i}{2} \left(\psi \frac{\partial \psi^*}{\partial t} - \psi^* \frac{\partial \psi}{\partial t} \right) - \frac{1}{2} \left| \frac{\partial \psi}{\partial x} \right|^2 + U(x) |\psi|^2 + \frac{g_s}{2} |\psi|^4. \quad (4)$$

Using the above Lagrangian density and the trial wave-function, we find the effective Lagrangian $L = \int \mathcal{L} dx$ of the quantum mechanical system. We begin by writing the total Lagrangian of the system as a sum of two terms, i.e., $L = L_c + L_{nc}$, where L_c represents the conservative term and L_{nc} defines the non-conservative term. The conservative part of the Lagrangian means that we only consider the real part of the external potential. While the non-conservative term describes the complex part of the external potential. By using the Lagrangian L , we deter-

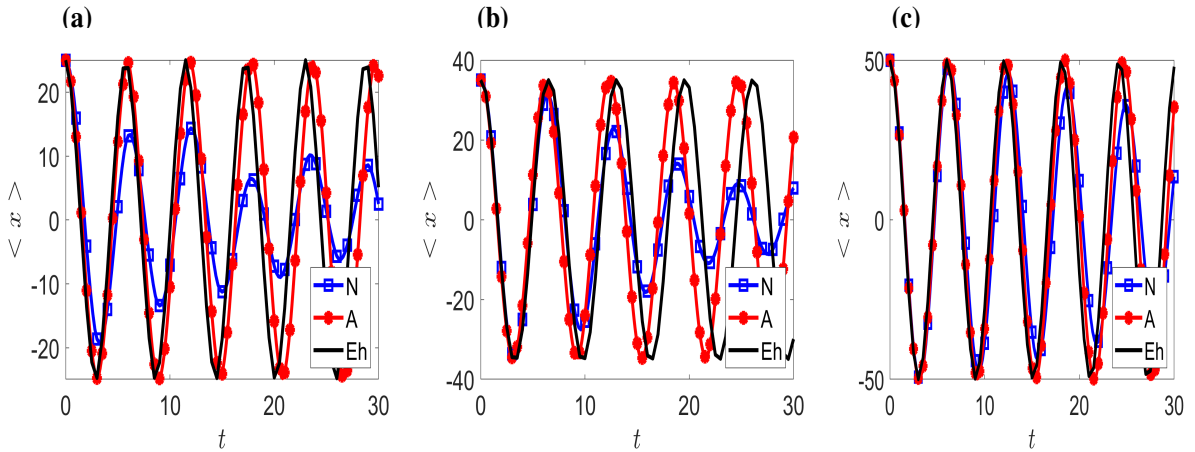


FIG. 3: (Color online) The dimensionless mean position of the *BEC* is plotted against the dimensionless time t for different initial mean position of the *BEC* $x_0 = 25$ (a), $x_0 = 35$ (b), and $x_0 = 50$ (c). The mean position is calculated by numerical (blue box), analytical (red circle), and Ehrenfest (black line) methods. Other dimensionless parameters are, $W_0 = 0$, $g_s = 3$, and the strength of the periodic potential is $V_0 = 30$.

mine the complex Ginzburg-Landau equation (CGLE) as [18, 25, 26]

$$\frac{d}{dt} \left(\frac{\partial L_c}{\partial \dot{s}} \right) - \frac{\partial L_c}{\partial s} = 2 \text{Re} \left[\int_{-\infty}^{\infty} iW(x)\psi^* \frac{\partial \psi}{\partial s} dx \right], \quad (5)$$

where s describe the set of dimensionless variational parameters such as, $x_0(t)$, $\alpha(t)$, $a(t)$, and $\beta(t)$. By using equation (4) and equation (5), we determine time-dependent equation for the dimensionless mean position of the *BEC*,

$$x_0''(t) + x_0(t) = V_0 \sin(2x_0(t))e^{-a^2(t)}, \quad (6)$$

here, we let $W(x) = 0$. While the dynamics of the width of the *BEC* analytically is given by

$$a''(t) + a(t) = \frac{1}{a^3(t)} + \frac{g_s}{\sqrt{2\pi}a^2(t)} + 2a(t)V_0 \cos(2x_0(t))e^{-a^2(t)}. \quad (7)$$

For above equations (6) and (7) we deliberately avoid to write the complex part of the potential, i.e., we have only consider the conservative L_c part of the Lagrangian while the "non-conservative" part makes our equations cumbersome, therefore, we avoid to present those lengthy equation here.

B. Ehrenfest method

The classical approximation of a quantum system can be realized by the Ehrenfest method [27],

$$\langle \ddot{x} \rangle = - \langle V'(x) \rangle, \quad (8)$$

Where $V(x)$ defines the trapping potential for the *BEC* wave packet and the Ehrenfest theorem leads to the dimensionless mean position of the *BEC* equation as

$$\langle \ddot{x} \rangle = - \langle x \rangle + 2V_0 \cos(\langle x \rangle) \sin(\langle x \rangle), \quad (9)$$

the mean position of the wave-packet is strongly depends on the optical lattice potential V_0 .

C. Numerical method

To solve numerically the quasi-1D GPE, we use the time-splitting spectral method [28] We choose time step as $\Delta t = 0.0001$, and a space step as $\Delta x = 0.0177$, to discretize the dimensionless quasi-1D GPE Eq. (1). To give a momentum kick to the *BEC* wave packet, initially we trap the *BEC* at potential $V(x) = (x - x_0)^2/2$, where x_0 defines the initial mean position of the *BEC*. Later, we switched off the trapping potential and switch the potential minimum to the new potential $V(x) = x^2/2 + V_0 \cos^2(x)$. In this way, *BEC* experience a kick and starts dipole oscillations in the left over potential.

III. BEC DYNAMICS

To study the dynamics of a *BEC* in this closed environment, we compare the analytical, Ehrenfest, and numerical methods discussed previously in Sec. II (A-C). First of all, the qualitative comparison of analytical and numerical results are presented in Fig. 1 in the form of a temporal density plot of the *BEC* in the absence of *PT*-symmetric potential. *BEC* dynamics applied under a *PT*-symmetric potential environment is presented in Fig. 5. We discuss both cases separately in the following two subsections.

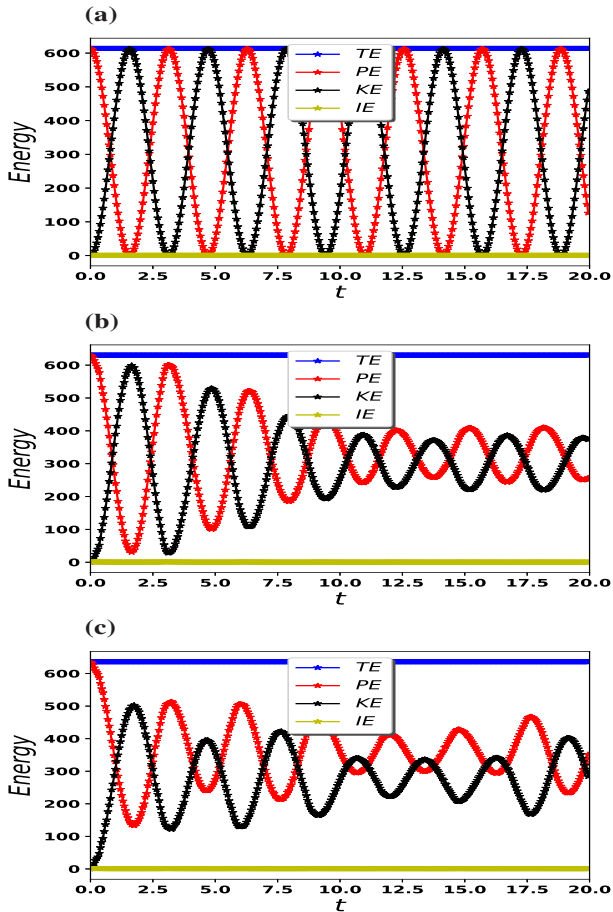


FIG. 4: (Color online) Energy evolution of a Bose-Einstein Condensate. Total energy is conserved in the whole process and kinetic energy and potential energy associated with harmonic trapping are evenly distributed at equilibrium. The parameters used are (a) $V_0 = 0$, (b) $V_0 = 30$, and (c) $V_0 = 40$.

A. Without PT -symmetric Potential

In this subsection, we compare and discuss the detailed result of the BEC dynamics without PT -symmetric potential, i.e., $W_0 = 0$, using analytical, Ehrenfest, and numerical methods.

1. Density dynamics of the BEC

The temporal density graph for the BEC is obtained numerically and analytically as shown in Fig. 1. For small values of the periodic potential strength, $V_0 = 5$, both analytical and numerical results are in agreement with each other as shown in Fig. 1(a-b). However, we observe that for higher values of the periodic potential strength, e.g., $V_0 = 50$, as presented in Fig. 1(c-d) both plots differ from each other. We note that the results obtained by the analytical method, Fig. 1(d), fails to reflect the physics of the dynamics of the BEC . Particularly, it shows no im-

part of scattering of the BEC due to the friction offered by the lattice potential. While the results obtained by the numerical method, Fig. 1(c), reveal the impact of the scattering from the peaks of the lattice potential and the dissipation. It reveals that quasi-particles are generated at the top of the BEC , which leads to thermalization of the BEC . So from now, for this section, we discuss only numerical results, because they present the real picture of the dynamics of the BEC .

For further investigation, we plot the mean position of the BEC , by using the numerical method as shown in Fig. 2. We observe that for periodic potential strength $V_0 = 0$ the BEC starts dipole oscillation without any dissipation in the closed environment as shown in Fig. 2. We note that for $V_0 = 30$, in Fig. 2, the numerical results show that the mean position of the BEC starts localizing at the global minima of the harmonic potential trap as presented in Fig. 2. For such a lattice potential the mean position dipole oscillation has a smaller amplitude. **For a larger value of the periodic potential, $V_0 = 100$ small BEC dipole oscillation can be seen as depicted in Fig. 2.** Initially, BEC starts moving towards the global minima of the external potential but on the way, it loses its energy and turns back, even without reaching the global minima of the potential and after some time it gets localized at local minima as shown in Fig. 2. This localization other than the global minima of the harmonic potential is due to the loss of the energy of the BEC by the periodic potential embedded on the harmonic potential. It is also quite surprising that the tunneling of the BEC is also suppressed in this special scenario, however, eventually, the BEC will localize to global minima but after a long time.

2. The mean position vs initial energy of the BEC

The qualitative comparison of the dimensionless mean position of the BEC is plotted in Fig. 3, for three different methods, numerical (N), analytical (A), and Ehrenfest (Eh). We compare the impact of the initial potential energy (PE) of the BEC on its dipole oscillations without any PT -symmetric environment. Under such condition, it is evident from the Fig. 3 that the initial potential energy of the BEC depends upon the choice of the initial mean position of the BEC , " x_0'' ". We know that the dimensionless potential energy is given by, $PE \propto x_0^2$. The initial energy of the BEC shows a considerable influence on the dipole oscillations as plotted in Fig. 3. In Fig. 3, we see the influence of initial energy on the dipole motion of the BEC for $x_0 = 25$, the numerical study shows that the dissipation of the BEC results in an earlier localization of the mean position of the BEC . On the other hand, for higher values of the magnitude of PE , say $x_0 = 50$, the BEC just experience the global harmonic potential and hence a to-and-fro motion results.

While the initial high PE compensates the periodic frictional potential. We note that for low initial potential energy, the BEC localized earlier as presented in Fig. 3. We also observe that the Ehrenfest and analytical methods could not capture the physics of the dimensionless mean-position of the BEC . As we do not find the dependence of the mean-position on the initial PE of the system, which is not physical. However, from the numerical calculation, we conclude that the initial high PE of the BEC results in a delay in the localization of the mean position of the BEC . We observe that the BEC with high PE maintains longer dipole oscillation for a longer time. Therefore, it is appropriate for experimentalists to consider this point while localizing the BEC . i.e., they must not put the BEC far away from the global minima, as it could lead to decoherence in the experiment, which could destroy the BEC . In a classical harmonic system, the total energy of the system is dissipative, due to the environment interaction, however, in our special case the system is isolated therefore the total energy is conserved as shown in Fig. 4. It means that periodic potential does not store energy during the thermalization process, however, periodic-potential distribute the energy, few other writers have also studied this phenomenon in disorder potentials [29]. As someone can see from Fig. 4 that for higher values of V_0 the kinetic energy (KE) and potential energy (PE) are oscillating, however, as time passes oscillation becomes smaller and smaller which leads to equilibrium. As a matter of fact, this energy distribution indicates another kind of non-equilibrium to an equilibrium state.

Since our system is in an isolated environment. So the localization is quite surprising in such a system. However, someone can answer this localization is due to the thermalization of the BEC . As the BEC is started to move from its initial position, it experiences friction in the system due to periodic potential. That periodic resistance generated quasi-particles at the top of the BEC , which can be seen in Fig. 1(c). This is not new as many studies already pointed out such quasi-particles due to the collision of the BEC wave-packet with external potentials [30].

B. With PT -Symmetric Environment

In this sub-section, we compare analytical and numerical BEC dynamics by observing the temporal density and the mean position of the BEC under a PT -symmetric environment. The amount of PT -symmetry or the imaginary part of the potential controlled by the parameter, W_0 .

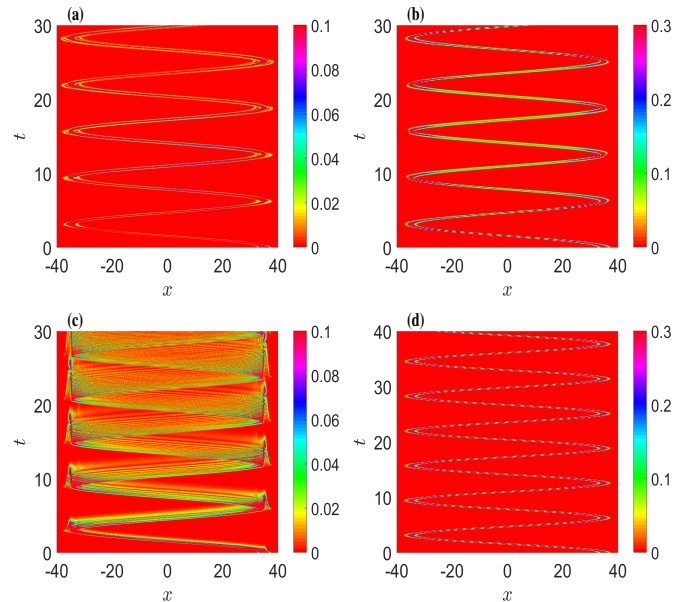


FIG. 5: (Color online) Comparison of numerical (left column) and analytical (right column) results of the BEC temporal density with a PT -symmetric potential. The dimensionless parameters defines as the interaction strength $g_s = 3$, initial mean position of the BEC $x_0 = 35$. The periodic potential strength for upper row is $V_0 = 5$ and the strength of the imaginary part of potential is $W_0 = 0.2$, while for the lower row the periodic potential strength is $V_0 = 30$ and the strength of the imaginary part of the potential is $W_0 = 0.2$.

1. The temporal density graph

The temporal density graph in Fig. 5 is obtained by analytical (right column) and numerical simulation (left column). Here, we note that for a small amount of PT -symmetry, $W_0 = 0.2$ and for a small amount of the strength of the external periodic potential, $V_0 = 5$, the analytically and numerically obtained results for the dynamics of the BEC are in good agreement. While there is disagreement in the results for higher values of the periodic potential strength, like $V_0 = 30$. For larger values of V_0 once again, we observe that the numerical results are in agreement with the physics of the dissipative dynamics and analytical methods are no longer valid.

2. Temporal mean position

In this subsection, we discuss the dynamics of the dimensionless mean position of the BEC , which is calculated by numerical method.

We observe that for small PT -symmetric potential the BEC shows the famous dipole oscillation, with a gradual decrease in dipole oscillation's amplitude as shown in Fig. 6. Which describes the localization of the BEC as already discussed in Sec. II. As we increase, the PT -

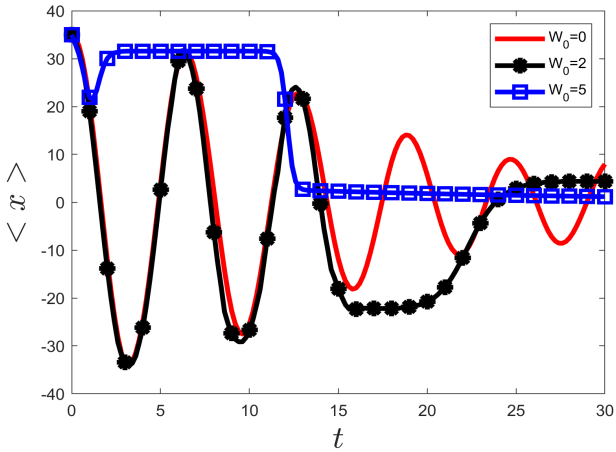


FIG. 6: (Color online) The impact of the amount of PT -symmetric potential on mean position of the BEC . The BEC initially located at $x_0 = 35$. Other dimensionless parameters are, $g_s = 3$, $V_0 = 30$.

symmetric potential " $W_0 = 2$ " we observe that the mean of the BEC starts dipole oscillation but around " $t = 15$ " we note that the dipole oscillation rapidly seized and the BEC localized at some local minima. However, as time passes the BEC mean position jumps to the global minima as predicted in Fig. 6. We realize that this jump is quite natural as in BEC particles are continuously ejected from the adjacent wells simultaneously. Additionally, there is a continuous compulsion for the BEC to move towards the global minima. As we raise the strength of the PT -symmetric to " $W_0 = 5$ " we inspect that the mean point of the BEC is localized around " $x = 30$ ", in a relatively short time as shown in Fig. 6. And it stays in this local minima for a relatively long time. Later, the mean position of the BEC switches towards the global minima. It is quite strange that we could not see the localization of the BEC in between the " $x = 30$ " and " $x = 0$ ". This is quite interesting as it leads to a kind of digital switching. So with this, we conclude that our proposed model can be used to study the localization of the BEC , additionally, it can also be used for discrete switching.

IV. CONCLUSION

In this paper, we compare the analytical, numerical, and Ehrenfest methods to study the BEC dynamics in a dissipative environment. Along with this, we also study the impact of the presence of the PT -symmetric on the dissipative dynamics of the BEC . The dissipative environment is created by adding a periodic potential over a harmonic potential. The dissipation is controlled by the strength of the periodic potential height. We conclude that the analytical and Ehrenfest methods have limita-

tions for larger values of the periodic potential strength, V_0 . For larger values of the periodic potential strength, the numerical methods remain valid. The presence of a periodic PT -symmetric environment influences the dynamics of the BEC in such a way that it can control the localization of the BEC at the desire location. By controlling the amount of PT -symmetric strength and the strength of the periodic potential parameter we can localize the BEC to a desirable location for a desirable time. **As a future prospective, someone can extend this work for spin-orbit coupled BEC 's [31] and for dipolar condensate [32, 33].**

V. ACKNOWLEDGMENT

Jameel Hussain gratefully acknowledges support from the COMSATS University Islamabad for providing him a workspace.

* Electronic address: javedakram@daad-alumni.de

- [1] M. H. Anderson, J. R. Ensher, M. R. Matthews, C. E. Wieman, and E. A. Cornell, *Science* **269**, 198 (1995).
- [2] K. B. Davis, M. O. Mewes, M. R. Andrews, N. J. van Druten, D. S. Durfee, D. M. Kurn, and W. Ketterle, *Phys. Rev. Lett.* **75**, 3969–3973 (1995).
- [3] C. C. Bradley, C. A. Sackett, and R. G. Hulet, *Phys. Rev. Lett.* **78**, 985–989 (1997).
- [4] D. G. Fried, T. C. Killian, L. Willmann, D. Landhuis, S. C. Moss, D. Kleppner, and T. J. Greytak, *Phys. Rev. Lett.* **81**, 3811–3814 (1998).
- [5] C. Raman, M. Köhl, R. Onofrio, D. S. Durfee, C. E. Kuklewicz, Z. Hadzibabic, and W. Ketterle, *Phys. Rev. Lett.* **83**, 2502–2505 (1999).
- [6] R. Onofrio, C. Raman, J. M. Vogels, J. R. Abo-Shaeer, A. P. Chikkatur, and W. Ketterle, *Phys. Rev. Lett.* **85**, 2228–2231 (2000).
- [7] K. W. Madison, F. Chevy, W. Wohlleben, and J. Dalibard, *Phys. Rev. Lett.* **84**, 806–809 (2000).
- [8] P. C. Haljan, I. Coddington, P. Engels, and E. A. Cornell, *Phys. Rev. Lett.* **87**, 210403 (2001).
- [9] E. Hodby, G. Hechenblaikner, S. A. Hopkins, O. M. Maragò, and C. J. Foot, *Phys. Rev. Lett.* **88**, 010405 (2001).
- [10] J. Akram and A. Pelster, *Phys. Rev. A* **93**, 023606 (2016).
- [11] J. Akram and A. Pelster, *Phys. Rev. A* **93**, 033610 (2016).
- [12] J. Akram and A. Pelster, *Laser Physics* **26**, 065501 (2016).
- [13] J. Hussain, J. Akram, and F. Saif, *Journal of Low Temperature Physics* **195**, 429–436 (2019).
- [14] J. Akram, *Laser Physics Letters* **15**, 025501 (2018).
- [15] A. Posazhennikova, M. Trujillo-Martinez, and J. Kroha, *Annalen der Physik* **530**, 1700124 (2018).
- [16] A. Polkovnikov, K. Sengupta, A. Silva, and M. Vengalattore, *Rev. Mod. Phys.* **83**, 863–883 (2011).
- [17] S. Trotzky, Y.-A. Chen, A. Flesch, I. P. McCulloch, U. Schollwöck, J. Eisert, and I. Bloch, *Nature Physics* **8**, 325–330 (2012).

- [18] J. Hussain, M. Nouman, F. Saif, and J. Akram, *Physica B: Condensed Matter* **587**, 412152 (2020).
- [19] C. M. Bender and S. Boettcher, *Phys. Rev. Lett.* **80**, 5243–5246 (1998).
- [20] L. Pítajevskij, L. S. Stringari, L. Pitaevskii, S. Stringari, S. Stringari, and O. U. Press, *Bose-Einstein Condensation*, International Series of Monographs on Physics (Clarendon Press, 2003).
- [21] D. Anderson, *Phys. Rev. A* **27**, 3135–3145 (1983).
- [22] V. M. Pérez-García, H. Michinel, J. I. Cirac, M. Lewenstein, and P. Zoller, *Phys. Rev. A* **56**, 1424–1432 (1997).
- [23] V. M. Pérez-García, H. Michinel, J. I. Cirac, M. Lewenstein, and P. Zoller, *Phys. Rev. Lett.* **77**, 5320–5323 (1996).
- [24] R. Borghi, *European Journal of Physics* , 035410.
- [25] I. S. Aranson and L. Kramer, *Rev. Mod. Phys.* **74**, 99–143 (2002).
- [26] L. Devassy, C. P. Jisha, A. Alberucci, and V. C. Kurikose, *Phys. Rev. E* **92**, 022914 (2015).
- [27] P. Ehrenfest, *Zeitschrift für Physik* , 455–457.
- [28] W. Bao, D. Jaksch, and P. A. Markowich, *Journal of Computational Physics* **187**, 318–342 (2003).
- [29] Y.-W. Hsueh, C.-H. Hsueh, and W.-C. Wu, *Entropy* **22** (2020), 10.3390/e22080855.
- [30] D. Dries, S. E. Pollack, J. M. Hitchcock, and R. G. Hulet, *Phys. Rev. A* **82**, 033603 (2010).
- [31] R. Liao, Y. Yi-Xiang, and W.-M. Liu, *Phys. Rev. Lett.* **108**, 080406 (2012).
- [32] A. R. P. Lima and A. Pelster, *Phys. Rev. A* **84**, 041604 (2011).
- [33] B. Nikolić, A. Balaz, and A. Pelster, *Phys. Rev. A* **88**, 013624 (2013).